Intercomparison of Electromagnetic Scattering Models for Delay-Doppler Maps along a CYGNSS Land Track with Topography

James Campbell [1], Ruzbeh Akbar [2], Alexandra Bringer [2], Davide Comite [2], Laura Dente [2], Scott Gleason [2], Leila Guerriero [2], Erik Hodges [2], Joel Johnson [2], Seungbum Kim [2], Amer Melebari [2], Nazzareno Pierdicca [2], Christopher Ruf [2], Leung Tsang [2], Tianlin Wang [2], Haokui Xu [2], Jiyue Zhu [2], and Mahta Moghaddam [2]

[1]University of Southern California
[2]Affiliation not available

October 30, 2023

Abstract

A comparison of three different electromagnetic scattering models for land surface delay-Doppler maps (DDMs) obtained from global navigation satellite system reflectometry (GNSS-R) along a Cyclone Global Navigation Satellite System (CYGNSS) track in the San Luis Valley, Colorado, USA, is presented. The three models are the analytical Kirchhoff solutions (AKS), the Soil And VEgetation Reflection Simulator (SAVERS), and the improved geometrical optics with topography (IGOT). Common inputs to the three models were defined by using field samples of soil moisture and texture, soil surface roughness measurements, and a digital elevation model (DEM). The resulting peak reflectivity profiles of the models and the CYGNSS data all had a dynamic range of 10 dB along the selected track, mainly due to the influence of topography. The reflectivities obtained from all three models agreed with one another to within 2.4 dB along the full length of the track. The models also showed general agreement with the corresponding CYGNSS data, although the modeled profiles were higher and smoother. Additional characterization of fine-scale surface roughness is identified as an area for future work to improve model fidelity. An intercomparison of DDM structure for three selected acquisitions is also provided.

Intercomparison of Electromagnetic Scattering Models for Delay-Doppler Maps along a CYGNSS Land Track with Topography

James D. Campbell, *Senior Member, IEEE,* Ruzbeh Akbar, *Member, IEEE,* Alexandra Bringer, *Member, IEEE,* Davide Comite, *Senior Member, IEEE,* Laura Dente, Scott T. Gleason, *Senior Member, IEEE,* Leila Guerriero, *Member, IEEE,* Erik Hodges, *Member, IEEE,* Joel T. Johnson, *Fellow, IEEE,* Seung-Bum Kim, Amer Melebari, *Graduate Student Member, IEEE,* Nazzareno Pierdicca, *Senior Member, IEEE,* Christopher S. Ruf, *Fellow, IEEE,* Leung Tsang, *Fellow, IEEE,* Tianlin Wang, *Member, IEEE,* Haokui Xu, *Graduate Student Member, IEEE,* Jiyue Zhu, *Student Member, IEEE,* and Mahta Moghaddam, *Fellow, IEEE*

***Abstract*—A comparison of three different electromagnetic scattering models for land surface delay-Doppler maps (DDMs) obtained from global navigation satellite system reflectometry (GNSS-R) along a Cyclone Global Navigation Satellite System (CYGNSS) track in the San Luis Valley, Colorado, USA, is presented. The three models are the analytical Kirchhoff solutions (AKS), the Soil And VEgetation Reflection Simulator (SAVERS), and the improved geometrical optics with topography (IGOT). Common inputs to the three models were defined by using field samples of soil moisture and texture, soil surface roughness measurements, and a digital elevation model (DEM). The resulting peak reflectivity profiles of the models and the CYGNSS data all had a dynamic range of 10 dB along the selected track, mainly due to the influence of topography. The reflectivities obtained from all three models agreed with one another to within 2.4 dB along the full length of the track. The models also showed general agreement with the corresponding CYGNSS data, although the modeled profiles were higher and smoother. Additional characterization of fine-scale surface roughness is identified as an area for future work to improve model fidelity. An intercomparison of DDM structure for three selected acquisitions is also provided.**

***Index Terms*—global navigation satellite system reflectometry (GNSS-R), land applications, scattering model, surface topography, Cyclone Global Navigation Satellite System (CYGNSS).**

Manuscript received XXXX; revised YYYY. This work was supported in part by the NASA Science Mission Directorate under Grant 80NSSC18K0704 with the University of Southern California and under Contract NNL13AQ00C with the University of Michigan. This work was also supported in part by the European Space Agency under Contract 4000130560/20/NL/FF/gp. This work was presented in part at the 2021 IEEE International Geoscience and Remote Sensing Symposium (IGARSS). *(Corresponding author: J. D. Campbell.)*

J. D. Campbell, E. Hodges, A. Melebari, and M. Moghaddam are with the Microwave Systems, Sensors, and Imaging Lab (MiXIL), Department of Electrical and Computer Engineering, University of Southern California, Los Angeles, CA, 90007 USA (e-mail: jamesc91@usc.edu, ehodges@usc.edu, amelebar@usc.edu, mahta@usc.edu).

R. Akbar is with the Department of Civil and Environmental Engineering, Massachusetts Institute of Technology, Cambridge, MA 02139 USA (e-mail: rakbar@mit.edu).

A. Bringer, J. T. Johnson, and T. Wang are with the Department of Electrical and Computer Engineering and ElectroScience Laboratory, The Ohio State University, Columbus, OH 43210 USA (e-mail: bringer.1@osu.edu; johnson.1374@osu.edu; wang.15085@osu.edu).

D. Comite and N. Pierdicca are with the Department of Information Engineering, Electronics and Telecommunications, La Sapienza University of Rome, Rome 00184, Italy (e-mail: davide.comite@uniroma1.it; nazzareno.pierdicca@uniroma1.it).

L. Dente and L Guerriero are with the Department of Civil Engineering and Computer Science Engineering, Tor Vergata University of Rome, Rome 00133, Italy (e-mail: laura.dente@uniroma2.it; leila.guerriero@uniroma2.it).

S. Gleason is with the Constellation Observing System for Meteorology, Ionosphere, and Climate (COSMIC) Program, University Corporation for Atmospheric Research (UCAR), Boulder, CO 80301 USA (e-mail: gleason@ucar.edu).

S.-B. Kim is with the Jet Propulsion Laboratory, California Institute of Technology, Pasadena, CA 91109 USA (email: seungbum.kim@jpl.nasa.gov).

C. S. Ruf is with the Department of Climate and Space Sciences and Engineering (CLASP), University of Michigan, Ann Arbor, MI 48109-2143 USA (e-mail: cruf@umich.edu).

L. Tsang, H. Xu, and J. Zhu are with the Radiation Laboratory, Department of Electrical Engineering and Computer Science, University of Michigan, Ann Arbor, MI 48109 USA (e-mail: leutsang@umich.edu; xuhaoku@umich.edu; jiyuezhu@umich.edu)

I. INTRODUCTION

REFLECTIONS of satellite signals from land surfaces are sensitive to a variety of biogeophysical parameters of interest for environmental monitoring from space [1]–[3]. With the proliferation of spaceborne global navigation satellite system reflectometry (GNSS-R) missions and experiments in recent years, there is a growing need for the development and validation of electromagnetic scattering models to describe the delay-Doppler map (DDM) data generated by these sensors.

This work provides an intercomparison of GNSS-R DDM models for a Cyclone Global Navigation Satellite System (CYGNSS) [4] track over a validation site in the San Luis Valley (SLV), Colorado, USA. As the validation site has little vegetation, the intercomparison focuses on modeling the effects of topography, microwave-scale surface roughness, and soil dielectric constant. The intercomparison includes the following three models:

- An implementation of the analytical Kirchhoff solutions (AKS) [5]
- The Soil And VEgetation Reflection Simulator (SAVERS) [6]
- An implementation of the improved geometrical optics with topography (IGOT) method [7]

Each of these models is based on the Kirchhoff integral, and each uses a different approach for its evaluation.

In addition to the three models and simulators identified above and studied in this work, another end-to-end simulator for spaceborne GNSS-R land applications that includes the effects of topography is SIM4Land, which grew out of the European Space Agency (ESA)-funded GNSS-R Assessment of Requirements and Consolidation of Retrieval Algorithms (GARCA) and GNSS REflectometry, Radio Occultation, and Scatterometry (GEROS) projects. Matchups between GARCA/GEROS-SIM4land and TDS-1 GNSS-R data, including a track with high topographic variation, have been reported in [8].

The present work originated with discussions among several of the coauthors at the CYGNSS Science Team Meeting held in Pasadena, CA, USA, in January 2020. The coauthors began to hold regular teleconferences to coordinate the model intercomparison effort later the same year. A preliminary version of this work was presented in July 2021 [9].

The methodology of the model intercomparison and the corresponding validation site are described in Section II. Results are presented in Section III and further discussed in Section IV.

II. Methodology

A. Summary of Models

Given the near-specular observations of GNSS-R systems, the physical optics approximation (or Kirchhoff approach) is expected to provide reasonable accuracy for predicting the scattering of a rough land surface under low vegetation conditions. The three models considered in this work all are fundamentally based on the Kirchhoff approximation for surface scattering. The models differ in their description of land surface roughness properties. Land surface roughness can occur over a variety of length scales, ranging from the millimeter- to centimeter-scale heights, known as microwave-scale roughness, that occur over the meter-scale baselines typically measured in situ, to the topographic roughness of meter-scale changes in heights among the $\sim$30 m or coarser spaced grid points of digital elevation models (DEMs), as well as intermediate-scale roughness occurring on horizontal length scales between $\sim$1 m and $\sim$30 m. Roughness on all of these scales can impact specular scattering and should therefore be characterized in any model to be applied. Note that information on intermediate-scale roughness is frequently unavailable, so that its effects can often be considered as a tuning parameter in the modeling process. The wide range of length scales involved motivates approaches that decouple prediction of the surface specular scattering with respect to the roughness length scale. The three models compared in this paper approach this decomposition in distinct ways. It is also noted that specular reflections from Earth's land surface can include coherent contributions, where reflections from many surface points add constructively at the receiver, and also incoherent contributions, where reflections have random phase, with coherent contributions being more likely in cases with extremely low surface roughness. The three models considered also have distinct means for treating coherent contributions.

1) AKS: In the AKS approach [5], the land surface terrain is represented by a three-scale surface model

$$f(x,y) = f_1(x,y) + f_2(x,y) + f_3(x,y) \tag{1}$$

where $f_1(x,y)$ and $f_3(x,y)$ represent the microwave and topographic scales, respectively, with the former described statistically using parameters from in-situ profile measurements, and the latter obtained from a 30 m DEM. The DEM elevations are used to construct 30 m tilted planar patches whose slopes are determined from the derivatives of $f_3(x,y)$. The $f_2(x,y)$ profile represents an intermediate scale of roughness, which is alternatively called fine-scale topography. Recently, light detection and ranging (lidar) measurements have been taken from which $f_2(x,y)$ can be reconstructed deterministically in the future. In this work, $f_3(x,y)$ is represented by deterministic planar patches, whereas both $f_1(x,y)$ and $f_2(x,y)$ are treated statistically. Let $f_{12}(x,y) = f_1(x,y) + f_2(x,y)$, which is the combination of microwave roughness and fine-scale topography. Stochastic descriptions for $f_1(x,y)$, $f_2(x,y)$, and $f_{12}(x,y)$ are given in [5]. Salient features of the AKS approach include:

- Analytical expressions are derived based on the Kirchhoff integral for both coherent and incoherent waves.
- Monte Carlo simulations are not required, making it computationally efficient.
- Analytical solutions are given in terms of the spectrum of $f_{12}(x,y)$.

In this approach, there is no need to divide microwave roughness and fine-scale topography, and the surface spectrum derived from lidar measurements can be incorporated directly. For both coherent and incoherent waves, the AKS approach gives results that are indistinguishable from the numerical Kirchhoff approach (NKA), which is a brute force accurate method that carries out the Kirchhoff integral directly using 2 cm discretization. Results show that $f_2(x,y)$ has significant effects [5].

To calculate the coherent waves for a certain area, the coherent field is first obtained from each 30 m DEM patch while accounting for the impact of the f_{12} roughness on the patch. Then, the total coherent field is obtained by the complex summation of the coherent field over patches and the absolute value squared is finally taken to find the coherent intensity of the area. For the incoherent waves, the incoherent intensity from each 30 m DEM patch is computed. Then, the total intensity is obtained by summation of all the contributions from patches. With calculated coherent and incoherent intensity, the total scattering from the area can be obtained [5].

2) SAVERS: SAVERS is based on the original formulation in [10], which was designed to simulate low altitude receivers. It was updated as described in [6] to include the topography of the illuminated area, which cannot be neglected at satellite altitude. To account for topography, the DEM derived from the Shuttle Radar Topography Mission (SRTM) is considered. Each DEM element is a facet with its individual orientation, above which the roughness at wavelength scale is superimposed.

SAVERS implements the integral bistatic radar equation [11], independently evaluating the incoherent diffuse and coherent near-specular scattering components. The former is computed through the advanced integral equation method (AIEM) [12], whereas the latter is simulated using the approach described in [13], which relies on the definition of a coherent normalized radar cross section (NRCS), associating a prescribed scattering pattern with the DEM facets. The beamwidth of the pattern of the coherent component is a parameter, denoted by β, that depends on the system geometry and configuration, such as frequency and distance. Since it drives the directivity of the quasi-specular scattering component [13], it can be connected to the effect of the intermediate-scale roughness on the patch NRCS angular pattern. In the SAVERS simulations performed in this study, the parameter β has been set to 0.03°, which is the same order of magnitude of the one retrieved in [13] for a satellite geometry.

SAVERS also includes a module for simulating vegetated areas, evaluating the scattering from forest and agricultural vegetation and setting the relevant geometric features of the vegetation elements through growth models. The modeling implements the radiative transfer equation, considering media constituted of randomly distributed scatterers representing different vegetation elements (namely, leaves, branches and trunks) [6]. The contributions of each DEM facet are combined through the radar equation considering the CYGNSS antenna pattern and the transformation between the local incidence and observation angles and polarization state going from the global reference frame linked to the instrument to the local facet reference frame and vice versa. In the work reported in this paper, the effects of vegetation are not included since the surfaces near the validation site were nearly bare at the time of data acquisition.

3) IGOT: The IGOT method, first described in [7], follows closely the approach of [11] with the assumption that the Rayleigh roughness parameter is large on the horizontal scale of the footprint of each delay-Doppler bin [14] so that coherent contributions vanish. Unlike [11], however, the IGOT surface height is considered to be not a purely random field but rather decomposed into a deterministic part obtained from a DEM and a random part representing the residual height between the DEM and the surface. The random part of surface height is further decomposed into a longwave process and a shortwave process, following the improved geometric optics model [15]. A derivation from first principles that includes the shortwave diffraction process is provided in the video presentation of [16]. Thus, the IGOT model is parameterized by

- DEM heights and gradients representing large-scale topography
- A root mean square (RMS) slope characterizing the roughness scale between the DEM resolution and the geometric optics cutoff
- An RMS height accounting for attenuation of the geometrical optics scattering due to shortwave diffraction

4) Discussion: The three models described have similar approaches for describing the microwave- and topographic-scale roughness, but all represent the intermediate-scale land roughness and treat coherent scattering contributions in distinct ways. The AKS model represents this roughness statistically in terms of an associated surface covariance function and computes the Kirchhoff expression for the surface NRCS without resorting to the geometrical optics approximation. The SAVERS model similarly requires knowledge of the surface covariance function for the diffuse incoherent component, and further invokes the beamwidth parameter in the evaluation of near-specular contributions. The IGOT model in contrast assumes that geometrical optics holds for all surface DEM patches, which implies an assumption regarding the amplitude of the intermediate-scale roughness RMS heights, so that description only of the RMS slopes of the patch roughness is required. The intercomparisons to be shown will provide insight into the applicability of these assumptions.

B. Calibration/Validation Site

The SLV of South Central Colorado, USA, was selected as the location of the first calibration and validation (cal/val) site for land applications of the CYGNSS mission, in part due to the elevation being sufficiently high to experience freeze-thaw cycles but not so high as to exceed the operating envelope of the instrument. Located at the headwaters of the Rio Grande near the northern limit of the CYGNSS coverage zone and surrounded by mountainous terrain, the SLV is generally flat and sandy with croplands as the dominant land cover.

Two Soil moisture Sensing Controller and oPtimal Estimator (SoilSCAPE) in-situ wireless sensor networks (WSNs) named Z1 and Z4, whose locations are shown in Fig. 1, were installed in the SLV in late October of 2019 [17]. The SoilSCAPE project, initially funded by the NASA Earth Science Technology Office (ESTO) Advanced Information Systems Technology (AIST) program, aims to provide surface-to-depth estimates of soil moisture on a local scale with optimal sampling [18], [19]. The locations of the two WSNs were selected such that both represent similar weather and climate conditions. The site Z1 is a flat open pasture, whereas Z4 samples more hilly terrain. Each SoilSCAPE WSN includes multiple battery-powered end devices (EDs), each located within a radius of 500 m of the local coordinator (LC). A total of four EDs were installed at Z1, and five at Z4. Each ED has four Teros-12 probes to measure soil moisture and soil temperature at depths of 5, 10, 20, and 30 cm every twenty minutes. Soil moisture information from the wireless EDs is transmitted and collected at the LC, then uploaded in near real-time to the project's data server at https://soilscape.usc.edu. Additionally, each site includes a weather station which reports air temperature, precipitation, and solar radiation measurements every twenty minutes.

C. Track Selection

Criteria for selection of a CYGNSS track for the model intercomparison included:

1) Time of acquisition around October 25-27, 2019, when field samples were collected
2) Readings from all SLV SoilSCAPE temperature sensors above freezing
3) At least one acquisition located within 5 km of Z1 or Z4

Item 1 was included so that soil moisture from oven-drying of the field samples could be used rather than soil moisture from the SoilSCAPE sensors, whose calibration was delayed due to restrictions related to COVID-19. Additionally, the water content of the vegetation at the time of the field samples was

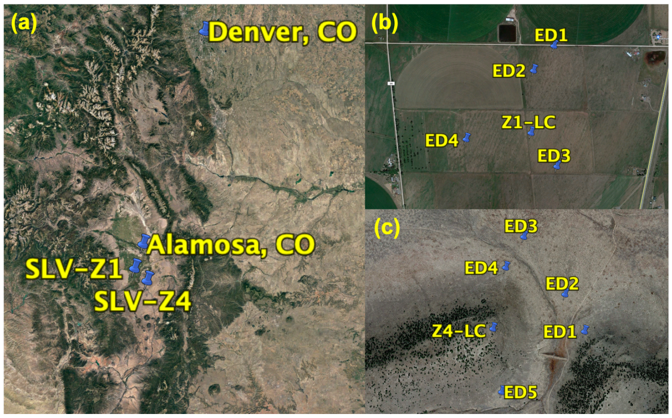

Figure 1. (a) Location of the SLV and the in-situ sensor sites Z1 and Z4. (b)-(c) Close-up view of Z1 (37.190°, −105.992°) and Z4 (37.060°, −105.820°) along with the location of individual wireless soil moisture end-nodes.

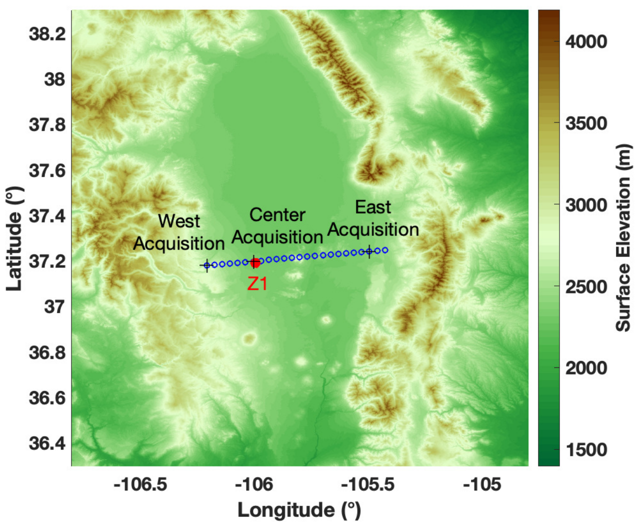

Figure 2. Reported CYGNSS specular points of selected track (blue circles), location of in-situ sensors at SLV site Z1 (red dot), and acquisitions selected for DDM shape comparison (black crosses) plotted over a map of topography.

observed to be low, which is aligned with this study's focus on sensitivity to topography rather than to land cover.

After analysis of CYGNSS data near these field samples, the track around 2019-10-28 14:04:58.5 UTC from channel 3 of spacecraft 2 was selected for this study as this track satisfied the three selection criteria above. The track, whose reported specular points are plotted over an elevation map in Fig. 2, passes over Z1, which has coordinates of (37.190°, −105.992°). The start and end of the track were determined by requiring CYGNSS signal-to-noise ratio (SNR) to be greater than 2 dB.

D. Soil Dielectric Constant

The soil moisture content measured from oven-drying of the Z1 field samples was $0.0259\,\mathrm{m^3\,m^{-3}}$. The clay fraction measured from the corresponding analysis of soil texture was 18 %. With these values of soil moisture and clay fraction, a soil dielectric constant of $2.987 + 0.173\,\mathrm{i}$ was calculated by the Mironov model [20], [21]. The same value was used by all three GNSS-R DDM models over the entire footprint of the selected track.

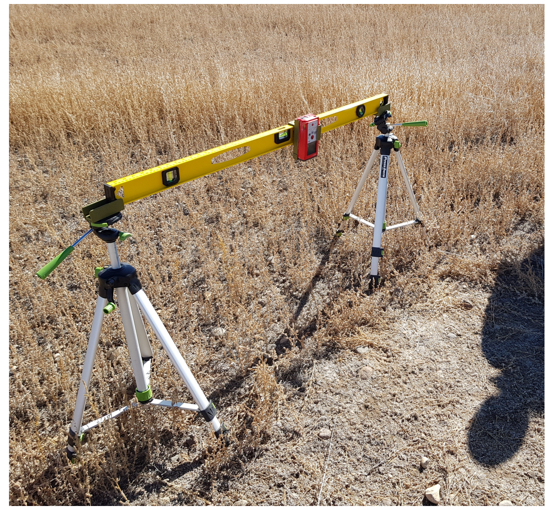

Figure 3. Special test equipment for measuring microwave-scale surface roughness: laser range finder that slides along a spirit level mounted on a pair of tripods. Photo by Amer Melabari.

E. Soil Surface Roughness

A laser range finder mounted on a spirit level supported by a tripod at each end, as shown in Fig. 3, was used to measure microwave-scale soil surface roughness along the baseline of the level at a total of thirteen locations and orientations around Z1, excluding a fourteenth measurement over a trench. Of the thirteen characterizations, seven used a baseline of approximately 0.5 m, and the other six had a baseline of approximately 1 m. Since the laser signal could reflect from vegetation, care was taken to avoid vegetated areas. The RMS of each characterization was computed relative to the mean for flat areas and relative to a linear regression for hilly locations. As shown in Fig. 4, a wide range of RMS values was observed. In particular, the values of RMS microwave scale surface roughness ranged from 0.23 to 2.65 cm with a median of 0.42 cm and a mean of 0.71 cm.

To further assess microwave-scale surface roughness, the field `bare_soil_roughness_retrieved` was extracted from the Soil Moisture Active Passive (SMAP) Level-3 product Radar Global Daily 3 km Equal Area Scalable Earth (EASE)-Grid Soil Moisture, Version 3 [22] for the week beginning July 1, 2015. This field is plotted against distance from Z1 in Fig. 5, which shows that points farther away from Z1 have a roughness value around 2 cm and sometimes higher, whereas the closest points have a roughness value around 0.5 cm. Using a radius of 3 km, the average roughness is 0.45 cm. A 5 km radius gives an average roughness of 1.03 cm, and an 8 km radius yields an average roughness of 1.48 cm. The increase in roughness with distance from Z1 is expected since Z1 is located in a relatively flat area that is surrounded by mountains. Note that the SMAP-derived roughness parameter is associated with a backscatter radar measurement at 40 degrees incidence angle, and therefore may not be completely applicable to describing near-specular surface scattering. The range of values

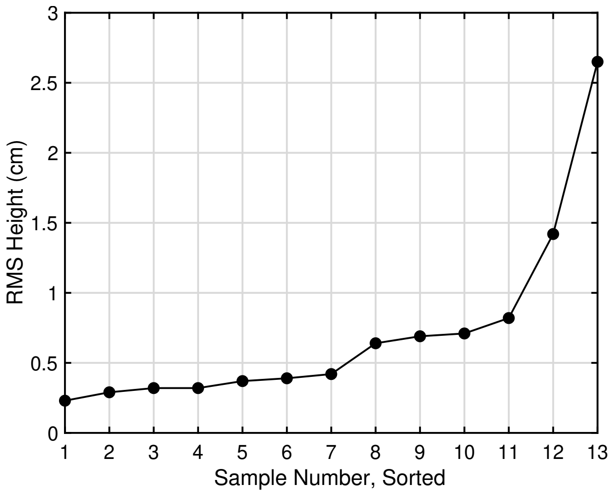

Figure 4. RMS surface roughness measured during fieldwork at Z1 in ascending order of magnitude.

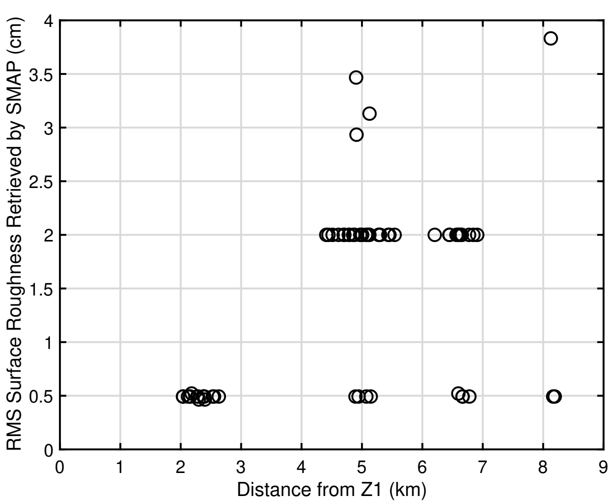

Figure 5. RMS surface roughness as estimated by SMAP within a radius of 9 km of Z1.

nevertheless provides some level of insight into roughness properties in this region.

In addition to RMS surface roughness retrieved by SMAP itself, RMS surface roughness from SMAP ancillary data [23] was examined, and the values over SLV were found to be about 1 cm.

In light of the data presented above on the microwave-scale soil surface roughness at Z1, the RMS height parameter was set to 1 cm for all three models. Since the AKS method represents f_1 not only by an RMS height parameter but also with a correlation function, an exponential correlation function with a correlation length of 10 cm was applied. The same correlation length was used in SAVERS for the incoherent component. These parameters were held constant over the entire footprint of the track selected for the reflectometry model intercomparison study of Section III-A and Section III-B.

Additionally, to help quantify the uncertainty introduced by variations in microwave-scale soil surface roughness, such as those observed in Fig. 4 and Fig. 5, a study of the sensitivity of one of the reflectometry models to soil surface RMS height is provided in Section III-C.

F. Surface Topography

All three models used the $1''$ SRTM DEM having approximately 30 m horizontal sampling for elevation. The models also used a common set of gradients estimated from the $1''$ SRTM DEM using linear least squares with a Hann window of size 15 by 15 samples. At the latitude of the SLV, this window corresponds to a region on the ground of approximately 370 by 460 m. The window size needed to be large enough to reduce the effects of noise from the SRTM product on the estimate of the gradients but not so large as to degrade their resolution. A comparison of results using two different window sizes for gradient estimation is provided in Section III-C.

The AKS and IGOT models both ran at the $1''$ resolution of the SRTM DEM, while SAVERS resampled to a spacing of $9''$, or approximately 300 m.

As described in Section II-A, all three models include parameters for characterizing surface roughness in the intermediate scale between the resolution of the DEM and the microwave scale. For this study, the AKS model represented f_2 by a Gaussian correlation function with RMS height of 5 cm and correlation length of 125 times the RMS height. The SAVERS simulation set β to 0.03°. The IGOT model was run with a relative RMS slope of 0.4°. These parameters were held fixed over the entire footprint of the selected track.

G. Antenna Pattern

In the interest of reproducibility from publicly available data, all three models used an isotropic antenna pattern. The convention for antenna gain is described in Section II-I. A comparison of results with isotropic and anisotropic (i.e., directional) antenna patterns is provided in Section III-C.

H. CYGNSS Data

Version 3.1 of the CYGNSS level 1 science data record was selected for comparison with the model results [24], [25]. This was the most recent version at the time of writing.

I. Conversion to Reflectivity

To facilitate meaningful comparisons among the model results and the CYGNSS data, a common convention for antenna gains and DDM units needed to be defined. Typically, DDMs are expressed in one of the following ways:

- Power in units of watts. Whereas this convention is valid for both coherent and incoherent reflections, it has no interpretation as a physical property of the reflecting surface.
- Bistatic radar cross section (BRCS) σ in units of square meters. This convention has physical significance for incoherent reflections, such as those from ocean surfaces, and it is used for the calibrated CYGNSS Level 1b (L1b) product [26].

- Normalized bistatic radar cross section (NBRCS) σ_0 in units of square meters per square meter. Having physical significance for incoherent reflections, this convention is used to average multiple BRCS bins together over their corresponding effective areas, as in [26].
- Surface reflectivity Γ [27, Section 2-8]. This convention has physical meaning for coherent reflections, and it has traditionally been used for land applications since the reflections in early tower-based and airborne GNSS-R experiments were primarily coherent. It is also being included in the CYGNSS land product [28].

For this study, the last alternative, surface reflectivity, was adopted for consistency with previous work. A convention for surface reflectivity is developed in the following to permit convenient comparison among the three models and CYGNSS data products.

Each of the three forward models considered in this study can be written in the form of the bistatic radar equation given by [26, eq. (1)]

$$P^{\mathrm{g,FM}}_{\hat{\tau},\hat{f}} = \frac{P^{\mathrm{T,FM}}\lambda^2}{(4\pi)^3} \times \iint_A \frac{G^{\mathrm{T,FM}}_{x,y}\sigma^0_{x,y}G^{\mathrm{R,FM}}_{x,y}}{(R^{\mathrm{R}}_{x,y})^2(R^{\mathrm{T}}_{x,y})^2}\Lambda^2_{\hat{\tau};x,y}S^2_{\hat{f};x,y}\,\mathrm{d}x\,\mathrm{d}y \quad (2)$$

where superscript FM has been added to emphasize certain factors that are specific to the forward models, as distinguished from corresponding factors in the L1b calibration. Here, $P^{\mathrm{g}}_{\hat{\tau},\hat{f}}$ is modelled power received after coherent processing at delay $\hat{\tau}$ and Doppler $\hat{f}$ by way of scattering of the global navigation satellite system (GNSS) source from the rough surface, P^{T} is transmit power, λ is wavelength, $(x, y) \in A$ are the variables of surface integration, A is the region of diffuse scattering, $G^{\mathrm{T}}_{x,y}$ and $G^{\mathrm{R}}_{x,y}$ are transmit and receive antenna gain patterns, respectively, as a function of (x, y), $R^{\mathrm{T}}_{x,y}$ is the distance from the transmitter to the surface at (x, y), and $R^{\mathrm{R}}_{x,y}$ is the distance from the surface at (x, y) to the receiver, $\sigma^0_{x,y}$ is NBRCS at the bistatic scattering geometry defined by the transmitter position, the surface at (x, y), and the receiver position, and $\Lambda_{\hat{\tau};x,y}$ and $S_{\hat{f};x,y}$ are the Woodward ambiguity functions (WAFs) in delay and Doppler, respectively.

For the AKS, (2) represents the incoherent component only. Since the coherent component of the AKS was found to be negligible for the track selected in this study, the coherent component is not included here. (Nevertheless, we note that the convention developed in the following can be extended in a straightforward manner to include a coherent component if necessary by replacing (2) with the corresponding equation for coherent power in terms of reflectivity.) In SAVERS, (2) is always applicable since it includes both the diffuse and near-specular component. Likewise, under the assumptions of IGOT, (2) obtains from first principles [7, eq. (42)].

Calibrated CYGNSS DDMs are provided in the NetCDF variable `brcs` with units of square meters. From [26, eq. (4)], these L1b BRCSs are computed by

$$\sigma^{\mathrm{L1b}}_{\hat{\tau},\hat{f}} = \frac{(4\pi)^3(R^{\mathrm{R}}_{\mathrm{SP}})^2(R^{\mathrm{T}}_{\mathrm{SP}})^2}{\lambda^2P^{\mathrm{T,L1b}}G^{\mathrm{T,L1b}}_{\mathrm{SP}}G^{\mathrm{R,L1b}}_{\mathrm{SP}}}P^{\mathrm{g,L1a}}_{\hat{\tau},\hat{f}} \quad (3)$$

where superscripts L1a and L1b have been added to emphasize certain factors that are specific to the calibration, as distinguished from the corresponding factors in the forward models, and where subscript SP denotes evaluation at the specular point reported by the L1b calibration. Here, $P^{\mathrm{g,L1a}}_{\hat{\tau},\hat{f}}$ is the measured power DDM in units of watts from the Level 1a (L1a) calibration.

Since (3) represents a CYGNSS version-specific convention for conversion from units of watts to units of square meters, the same convention can also be used to convert a forward model result from units of watts (whether coherent or incoherent) to units of square meters for comparison with a particular version of L1b CYGNSS data

$$\sigma^{\mathrm{FM}}_{\hat{\tau},\hat{f}} = \frac{(4\pi)^3(R^{\mathrm{R}}_{\mathrm{SP}})^2(R^{\mathrm{T}}_{\mathrm{SP}})^2}{\lambda^2P^{\mathrm{T,L1b}}G^{\mathrm{T,L1b}}_{\mathrm{SP}}G^{\mathrm{R,L1b}}_{\mathrm{SP}}}P^{\mathrm{g,FM}}_{\hat{\tau},\hat{f}} \quad (4)$$

Substituting (2) into (4), we obtain

$$\sigma^{\mathrm{FM}}_{\hat{\tau},\hat{f}} = \frac{(R^{\mathrm{R}}_{\mathrm{SP}})^2(R^{\mathrm{T}}_{\mathrm{SP}})^2P^{\mathrm{T,FM}}}{P^{\mathrm{T,L1b}}G^{\mathrm{T,L1b}}_{\mathrm{SP}}G^{\mathrm{R,L1b}}_{\mathrm{SP}}} \times \iint_A \frac{G^{\mathrm{T,FM}}_{x,y}\sigma^0_{x,y}G^{\mathrm{R,FM}}_{x,y}}{(R^{\mathrm{R}}_{x,y})^2(R^{\mathrm{T}}_{x,y})^2}\Lambda^2_{\hat{\tau};x,y}S^2_{\hat{f};x,y}\,\mathrm{d}x\,\mathrm{d}y \quad (5)$$

Approximating the range losses and the antenna gains inside the integral by their values at the specular point, we find

$$\sigma^{\mathrm{FM}}_{\hat{\tau},\hat{f}} = \frac{P^{\mathrm{T,FM}}G^{\mathrm{T,FM}}_{\mathrm{SP}}G^{\mathrm{R,FM}}_{\mathrm{SP}}}{P^{\mathrm{T,L1b}}G^{\mathrm{T,L1b}}_{\mathrm{SP}}G^{\mathrm{R,L1b}}_{\mathrm{SP}}} \times \iint_A \sigma^0_{x,y}\Lambda^2_{\hat{\tau};x,y}S^2_{\hat{f};x,y}\,\mathrm{d}x\,\mathrm{d}y \quad (6)$$

In the following, we adopt the conventions

$$\begin{aligned} P^{\mathrm{T,FM}} &= P^{\mathrm{T,L1b}} \\ G^{\mathrm{T,FM}}_{\mathrm{SP}} &= G^{\mathrm{T,L1b}}_{\mathrm{SP}} \\ G^{\mathrm{R,FM}}_{\mathrm{SP}} &= G^{\mathrm{R,L1b}}_{\mathrm{SP}} \end{aligned} \quad (7)$$

so that (6) becomes

$$\sigma^{\mathrm{FM}}_{\hat{\tau},\hat{f}} = \iint_A \sigma^0_{x,y}\Lambda^2_{\hat{\tau};x,y}S^2_{\hat{f};x,y}\,\mathrm{d}x\,\mathrm{d}y \quad (8)$$

Since (8) is independent of calibration-specific factors, this convention allows a single run of a forward model to be compared with multiple versions of CYGNSS L1b data. The convention also eliminates the need to favor any particular version of effective isotropic radiated power (EIRP) and receive antenna gain in the forward model run when comparing with multiple versions of CYGNSS L1b data.

Finally, to convert BRCS to reflectivity, we use the relationship

$$\Gamma_{\hat{\tau},\hat{f}} = \frac{1}{4\pi}\frac{(R^{\mathrm{R}}_{\mathrm{SP}}+R^{\mathrm{T}}_{\mathrm{SP}})^2}{(R^{\mathrm{R}}_{\mathrm{SP}})^2(R^{\mathrm{T}}_{\mathrm{SP}})^2}\sigma_{\hat{\tau},\hat{f}} \quad (9)$$

both for forward model results and for CYGNSS data. This relationship follows directly from (4) and the Friis formula for reflections [27, Section 5-10.5]. Here, the relationship is effectively independent of CYGNSS version since the relative difference in the reported ranges of the specular point between two versions is small.

Figure 6. Comparison of peak re ectivity from the three models and the corresponding CYGNSS level 1 science data along the selected track.

Table I
ACQUISITIONS SELECTED FOR DDM SHAPE COMPARISON

Identi er	Acquisition Time (UTC)	Specular Point Latitude (°)	Specular Point Longitude (°)
West	14:04:55.5	37.179	106.207
Middle	14:04:58.5	37.197	106.003
East	14:05:06.0	37.242	105.493

III. RESULTS

A. Along-Track Analysis

A comparison of peak re ectivity along the selected track is shown in Fig. 6. The horizontal axis is expressed in units of longitude so that each value of re ectivity can be associated with its corresponding reported specular point in Fig. 2. The plot also includes surface elevation at the specular points.

The re ectivity pro le of all three models and of the CYGNSS data is highest over the valley oor and decreases in the mountainous terrain on either side, and to a lesser degree over some hilly terrain in the middle, with a dynamic range of 10 dB.

All three models agree with one another to within 2.4 dB over the entire track. However, all three models overestimate version 3.1 of the CYGNSS data. In particular, the average of the three models is 5.0 dB higher than version 3.1 when averaged along the track. Furthermore, all three models appear to be generally smoother than the CYGNSS data.

B. Selected DDM Matchups

A comparison of DDMs for the three acquisitions identi ed in Table I from the selected track is shown in Fig. 7. The west acquisition has a positive Doppler tail. The middle acquisition is relatively compact in delay with a weak positive Doppler tail. The east acquisition has a negative Doppler tail. These structures are represented in both the CYGNSS data and the three models. Interpretation of the observed structures is provided in Section IV.

(a) West acquisition: AKS
(b) West acquisition: SAVERS
(c) West acquisition: IGOT
(d) West acquisition: CYGNSS
(e) Middle acquisition: AKS
(f) Middle acquisition: SAVERS
(g) Middle acquisition: IGOT
(h) Middle acquisition: CYGNSS
(i) East acquisition: AKS
(j) East acquisition: SAVERS
(k) East acquisition: IGOT
(l) East acquisition: CYGNSS

Figure 7. Comparison of DDMs from the three models and from the corresponding CYGNSS level 1 science data for the selected acquisition. Each DDM is normalized to its peak value to facilitate intercomparison of delay-Doppler structure. The units of the color map are decibels relative to the peak.

[13] D. Comite, F. Ticconi, L. Dente, L. Guerriero, and N. Pierdicca, "Bistatic coherent scattering from rough soils with application to GNSS reflectometry," *IEEE Trans. Geosci. Remote Sens.*, vol. 58, no. 1, pp. 612–625, Jan. 2020, doi:10.1109/tgrs.2019.2938442.

[14] A. M. Balakhder, M. M. Al-Khaldi, and J. T. Johnson, "On the coherency of ocean and land surface specular scattering for GNSS-R and signals of opportunity systems," *IEEE Trans. Geosci. Remote Sens.*, vol. 57, pp. 10 426–10 436, 2019, doi:10.1109/TGRS.2019.2935257.

[15] D. Thompson, T. Elfouhaily, and J. Garrison, "An improved geometrical optics model for bistatic GPS scattering from the ocean surface," *IEEE Trans. Geosci. Remote Sens.*, vol. 43, no. 12, pp. 2810–2821, Dec. 2005, doi:10.1109/tgrs.2005.857895.

[16] J. D. Campbell, A. Melebari, E. Hodges, R. Akbar, and M. Moghaddam, "Initial investigation of a GNSS-R multiscale rough surface forward model at San Luis Valley calibration/validation sites," in *2021 International Conference on Electromagnetics in Advanced Applications (ICEAA)*. IEEE, Aug. 2021, doi:10.1109/iceaa52647.2021.9539759.

[17] R. Akbar, J. Campbell, A. R. Silva, R. Chen, A. Melebari, E. Hodges, D. Entekhabi, C. Ruf, and M. Moghaddam, "SoilSCAPE wireless in situ networks in support of CYGNSS land applications," in *IEEE International Geoscience and Remote Sensing Symposium (IGARSS)*, Sep. 2020, doi:10.1109/igarss39084.2020.9324648.

[18] M. Moghaddam, D. Entekhabi, Y. Goykhman, K. Li, M. Liu, A. Mahajan, A. Nayyar, D. Shuman, and D. Teneketzis, "A wireless soil moisture smart sensor web using physics-based optimal control: Concept and initial demonstrations," *IEEE J. Sel. Topics Appl. Earth Observ. Remote Sens.*, vol. 3, no. 4, pp. 522–535, Dec. 2010, doi:10.1109/jstars.2010.2052918.

[19] M. Moghaddam, A. Silva, D. Clewley, R. Akbar, S. A. Hussaini, J. Whitcomb, R. Devarakonda, R. Shrestha, R. B. Cook, G. Prakash, S. S. Vannan, and A. G. Boyer, "Soil moisture profiles and temperature data from SoilSCAPE sites, USA," 2016, doi:10.3334/ORNLDAAC/1339.

[20] V. L. Mironov, M. C. Dobson, V. H. Kaupp, S. Komarov, and V. N. Kleshchenko, "Generalized refractive mixing dielectric model for moist soils," *IEEE Trans. Geosci. Remote Sens.*, vol. 42, no. 4, pp. 773–785, Apr. 2004, doi:10.1109/tgrs.2003.823288.

[21] V. L. Mironov, L. G. Kosolapova, and S. V. Fomin, "Physically and mineralogically based spectroscopic dielectric model for moist soils," *IEEE Trans. Geosci. Remote Sens.*, vol. 47, no. 7, pp. 2059–2070, Jul. 2009, doi:10.1109/tgrs.2008.2011631.

[22] S.-B. Kim, J. van Zyl, S. Dunbar, E. Njoku, J. Johnson, M. Moghaddam, J. Shi, and L. Tsang, "SMAP L3 radar global daily 3 km EASE-grid soil moisture, version 3," 2016, doi:10.5067/IGQNPB6183ZX.

[23] J. Peng, P. Mohommed, J. Chaubell, S. Chan, S. Kim, N. Das, S. Dunbar, R. Bindlish, and X. Xu, "Soil Moisture Active Passive (SMAP) L1-L3 ancillary static data, version 1," 2019, doi:10.5067/HB8BPJ13TDQJ.

[24] CYGNSS, "CYGNSS level 1 science data record version 3.1," 2021, doi:10.5067/CYGNS-L1X31.

[25] C. Ruf, S. Asharaf, R. Balasubramaniam, S. Gleason, T. Lang, D. McKague, D. Twigg, and D. Waliser, "In-orbit performance of the constellation of CYGNSS hurricane satellites," *Bulletin of the American Meteorological Society*, vol. 100, no. 10, pp. 2009–2023, Oct. 2019, doi:10.1175/bams-d-18-0337.1.

[26] S. Gleason, "Level 1B DDM calibration algorithm theoretical basis document," CYGNSS Project Document 148-0137, Rev 4, 09 Nov. 2021, https://podaac-tools.jpl.nasa.gov/drive/files/allData/cygnss/L1/docs/148-0137_ATBD_L1B_DDM_Calibration_R4.pdf, accessed Jan. 16, 2022.

[27] F. T. Ulaby and D. G. Long, *Microwave Radar and Radiometric Remote Sensing*. Ann Arbor, MI, USA: Univ. Michigan Press, 2014.

[28] S. Gleason, A. O'Brien, A. Russel, M. M. Al-Khaldi, and J. T. Johnson, "Geolocation, calibration and surface resolution of CYGNSS GNSS-R land observations," *Remote Sensing*, vol. 1317, no. 12, Apr. 2020, doi:10.3390/rs12081317.

[29] CYGNSS, "CYGNSS level 1 science data record version 2.1," 2017, doi:10.5067/CYGNS-L1X21.

[30] S. Gleason, M. M. Al-Khaldi, C. Ruf, D. S. McKague, T. Wang, and A. Russel, "Characterizing and mitigating digital sampling effects on the CYGNSS level 1 calibration," *IEEE Trans. Geosci. Remote Sens.*, 2021, early access, doi:10.1109/tgrs.2021.3120026.

[31] CYGNSS, "CYGNSS level 1 science data record version 3.0," 2020, doi:10.5067/CYGNS-L1X30.

James D. Campbell (Senior Member, IEEE) was born in Puyallup, WA, USA, in 1976. He received the B.S. degree in mathematics from Harvey Mudd College, Claremont, CA, USA, in 1998, the M.S. degree in applied mathematics from the California State Polytechnic University, Pomona, CA, USA, in 2006, and the Ph.D. degree in electrical engineering from the University of Southern California, Los Angeles, CA, USA, in 2019.

He is a Systems Engineer with Raytheon Intelligence and Space in El Segundo, CA, USA. He also has a part-time position with the Department of Electrical and Computer Engineering at the University of Southern California. He has previously worked with Wilson Campbell Systems in Anaheim, CA, USA, Dynamics Technology, Inc. in Torrance, CA, USA, and Boeing Integrated Shipboard Systems in Anaheim, CA, USA.

Dr. Campbell has been a member of the IEEE Geoscience and Remote Sensing Society (GRSS) since 2013. He has been co-leading the GNSS-R Working Group of the GRSS Modeling in Remote Sensing Technical Committee (MIRS TC) since 2021.

Ruzbeh Akbar (Senior Member, IEEE) earned the B.S. degree from the George Washington University (Summa Cum Laude), Washington, DC, USA, the M.S. degree from the University of Michigan, Ann Arbor, MI, USA, and the Ph.D. degree from the University of Southern California, Los Angeles, CA, USA, all in electrical engineering. He was the receipt of the NASA Earth and Space Fellowship (NESSF) in 2010. He is currently a Research Scientist in the Department of Civil and Environmental Engineering at the Massachusetts Institute of Technology, Cambridge, MA, USA. His research interests include applied electromagnetics, microwave remote sensing of Earth, hydrology, and wireless sensor networks. He is a member of the NASA-ESTO New Observation Strategies working group.

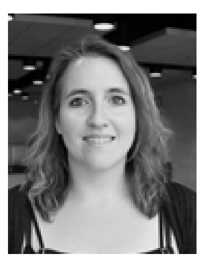

Alexandra Bringer (Member, IEEE) earned the M.S. degree and the Ph.D. degree in physics from the Université du Sud-Toulon-Var, La Garde, France, in 2009 and 2012, respectively. Her studies were focused on physical oceanography and remote sensing.

She joined the Electroscience Laboratory at The Ohio State University, Columbus, OH, USA, as a Research Scientist in 2014. Since then, she is working on microwave remote sensing for Earth monitoring.

Dr. Bringer is currently a science team member for the SMAP mission and the CYGNSS mission, and she is part of the soil moisture group for the NASA-ISRO Synthetic Aperture Radar (NISAR) mission. Her main research interests are Earth monitoring, microwave active and passive remote sensing for land, ocean and cryosphere applications and signal processing. She is also the chair of the IEEE Columbus Chapter Antennas and Propagation Society (AP-S)/Microwave Theory and Techniques Society (MTT-S) Joint Section and a member of the IEEE GRSS Frequency Allocations in Remote Sensing Technical Committee (FARS TC).

Davide Comite (Senior Member, IEEE) received the M.S. degree in communications engineering and the Ph.D. degree in electromagnetics and mathematical models for engineering from Sapienza University, Rome, Italy, in 2011 and 2015, respectively.

He was a Visiting Ph.D. Student with the Institute of Electronics and Telecommunications of Rennes, University of Rennes 1, Rennes, France, in 2014, and a Post-Doctoral Researcher with the Center of Advanced Communications, Villanova University, Villanova, PA, USA, in 2015. He is currently an Assistant Professor with Sapienza University. His research interests include the study of scattering from natural surfaces, GNSS-R, and the application of radar altimeters over land. He is also interested in the study and design of leaky-wave antennas and the generation of nondiffracting waves and pulses.

Dr. Comite is a senior member of the International Union of Radio Science (URSI) and IEEE. He is associate editor of the *Institution of Engineering and Technology (IET) Journal of Engineering*, the *IET Microwaves, Antennas and Propagation*, the IEEE ACCESS, and the IEEE JOURNAL OF SELECTED TOPICS IN APPLIED EARTH OBSERVATION AND REMOTE SENSING. He has been leading the GNSS-R Working Group of the GRSS MIRS TC since 2021.

Laura Dente received the Laurea degree in Physics from the University of Bari, Italy, in 2000 and the Ph.D. degree from the University of Twente, Netherlands, in 2016.

In 2002 she worked as a Young Graduate Trainee at the European Space Research and Technology Centre (ESTEC), Netherlands, and from 2003 to 2006 as a Research Fellow at the National Research Council (CNR) Institute of Intelligent Systems for Automation (ISSIA), Italy, on soil moisture and biomass retrieval from synthetic aperture radar (SAR) data. From 2007 to 2012 she was a Trainee Research Assistant at the University of Twente as International Institute for Geo-Information Science and Earth Observation (ITC) faculty, focusing on passive and active microwave remote sensing for soil moisture monitoring. Since 2016 she is a Research Fellow at the University of Rome Tor Vergata, where her main interests are GNSS-R and its application over land.

Scott T. Gleason (Senior Member, IEEE) received the B.S. degree in electrical and computer engineering from the State University of New York at Buffalo, Buffalo, NY, USA, in 1991, the M.S. degree in engineering from Stanford University, Stanford, CA, USA, in 1999, and the Ph.D. degree in applied physics from the University of Surrey, Surrey, UK, in 2007.

He is a Project Scientist with the University Corporation for Atmospheric Research, Boulder, CO, USA. He is a Co-Investigator on the science team and Instrument Scientist for the NASA CYGNSS Mission. He has worked in the areas of astronautics, remote sensing, and global navigation satellite systems for more than 20 years, including at NASA's Goddard Space Flight Center, Greenbelt, MD, USA; Stanford's GPS Laboratory, Stanford, CA, USA; Surrey Satellite Technology Ltd, Guildford, UK; Concordia University, Montréal, QC, Canada; and the National Oceanography Centre, Southampton, UK.

Leila Guerriero (Member, IEEE) received the Laurea degree in physics from Sapienza University, Rome, Italy, in 1986, and the Ph.D. degree in electromagnetism from Tor Vergata University, Rome, Italy, in 1991.

Since 1994, she has been a Permanent Researcher with Tor Vergata University, where she is currently an Associate Professor holding the courses on Earth satellite observation and on geoinformation. Her research interests include modeling microwave scattering and emissivity from agricultural and forested areas. She participated in several international projects, among them: the ESA projects Soil Moisture and Ocean Salinity Satellite, Development of SAR Inversion Algorithms for Land Applications, Use of Bistatic Microwave Measurements for Earth Observation, and Microwaves Observation Satellite-Companion Satellite (SAOCOM-CS) Bistatic Imaging, Radiometry and Interferometry over Land. Lately, she has been involved in the modeling of GNSS-R signals for ESA projects and in the European FP7 and H2020 Programmes.

Prof. Guerriero is a member of the Permanent Steering Scientific Committee of MicroRad. She is Secretary and Treasurer of the GRSS North-Central Italy Chapter.

Erik Hodges (Student Member, IEEE) received the B.S. degree in electrical engineering from the University of California Los Angeles, Los Angeles, CA, USA, in 2019. He is currently working toward the Ph.D. degree in electrical engineering at the University of Southern California, Los Angeles, CA, USA. He is a member of the CYGNSS Science Team and the IEEE GRSS. His research interests include GNSS-R and electromagnetic models for land surfaces.

Joel T. Johnson (Fellow, IEEE) received the bachelor of electrical engineering degree from the Georgia Institute of Technology, Atlanta, GA, USA, in 1991 and the S.M. and Ph.D. degrees from the Massachusetts Institute of Technology, Cambridge, MA, USA, in 1993 and 1996, respectively.

He is currently the Burn and Sue Lin Professor in the Department of Electrical and Computer Engineering and ElectroScience Laboratory of The Ohio State University, Columbus, OH, USA. His research interests are in the areas of microwave remote sensing, propagation, and electromagnetic wave theory.

Dr. Johnson is an IEEE Fellow, a member of Commissions B and F of URSI, and a member of Tau Beta Pi, Eta Kappa Nu, and Phi Kappa Phi. He received the 1993 best paper award from the IEEE GRSS, was named an Office of Naval Research Young Investigator, National Science Foundation Career awardee, and Presidential Early Career Award for Scientists and Engineers (PECASE) award recipient in 1997, and was recognized by the U.S. National Committee of URSI as a Booker Fellow in 2002.

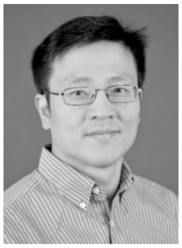

Seung-Bum Kim received the B.S. degree in electrical engineering from the Korea Advanced Institute of Science and Technology in 1992 and the M.S. and Ph.D. degrees in remote sensing from the University College London, England, in 1993 and 1998, respectively.

He has been with the Jet Propulsion Laboratory, Pasadena, CA, USA, since 2009. He was previously a Scientist at Remote Sensing Systems, California, USA, studying the L-band radiometry for the Aquarius salinity observation. His research interests currently includes microwave modeling and soil moisture retrieval with radar. Dr. Kim has been a member of the Aquarius, SMAP, and NISAR science teams.

Amer Melebari (Graduate Student Member, IEEE) was born in Jeddah, Saudi Arabia, in 1990. He received the B.S. degree in electrical and computer engineering with first-class honors from King Abdulaziz University, Jeddah, Saudi Arabia, in 2013 and the M.S. degree in electrical and computer engineering from the University of Southern California, Los Angeles, CA, USA, in 2019. He is currently working toward the Ph.D. degree in electrical engineering with the University of Southern California, Los Angeles, CA, USA.

He has been a Researcher with King Abdulaziz City for Science and Technology, Riyadh, Saudi Arabia, since 2013,

Amer Melebari has been a member of the IEEE GRSS since 2019.

Nazzareno Pierdicca (Senior Member, IEEE) received the Laurea (Doctorate) degree in electronic engineering (cum laude) from Sapienza University, Rome, Italy, in 1981.

From 1978 to 1982, he was with the Italian Agency for Alternative Energy, and from 1982 to 1990, with Remote Sensing Division, Telespazio, Rome, Italy. In November 1990, he joined the Department of Information Engineering, Electronics, and Telecommunications, Sapienza University of Rome. He is currently a Full Professor of remote sensing, antenna, and electromagnetic fields with the Faculty of Engineering, Sapienza University of Rome. His research interests include electromagnetic scattering and emission models for sea and bare soil surfaces and their inversion, microwave radiometry of the atmosphere, radar land applications, and bistatic radar.

Dr. Pierdicca is the Chair of the GRSS MIRS TC and a past Chairman of the GRSS Central Italy Chapter.

Christopher S. Ruf (Fellow, IEEE) received the B.A. degree in physics from Reed College, Portland, OR, USA, in 1982, and the Ph.D. degree in electrical and computer engineering from the University of Massachusetts at Amherst, Amherst, MA, USA, in 1987.

He has worked previously at Intel Corporation, Mountain View, CA, USA, Hughes Space and Communication, El Segundo, CA, USA, the NASA Jet Propulsion Laboratory, Pasadena, CA, USA, and Pennsylvania State University, University Park, PA, USA. He is the Frederick Bartman Collegiate Professor of climate and space science with the University of Michigan, Ann Arbor, MI, USA, and a Principal Investigator of the NASA CYGNSS mission. His research interests include GNSS-R remote sensing, microwave radiometry, atmosphere and ocean geophysical retrieval algorithm development, and sensor technology development.

Dr. Ruf is a member of the American Geophysical Union (AGU), the American Meteorological Society (AMS), and Commission F of the URSI. He is a former Editor-in-Chief of the IEEE TRANSACTIONS ON GEOSCIENCE AND REMOTE SENSING and has served on the editorial boards of the *Radio Science* and the *Journal of Atmospheric and Oceanic Technology*. He was a recipient of four NASA Certificates of Recognition and seven NASA Group Achievement Awards, as well as the 1997 TGRS Best Paper Award, the 1999 IEEE Resnik Technical Field Award, the 2006 IGARSS Best Paper Award, and the 2014 IEEE GRSS Outstanding Service Award.

Leung Tsang (Fellow, IEEE) was born and completed High School in Hong Kong. He received the B.S. degree, the M.S. degree, and the Ph.D. degree from the Massachusetts Institute of Technology, Cambridge, MA, USA.

He was with the University of Washington, Seattle, WA, USA, from 1983 to 2014 and was the Chair of the Electrical Engineering Department from 2006 to 2011. From 2001 to 2004, he was on leave at the Electrical Engineering Department of the City University of Hong Kong. Since January 2015, he has been a Professor with the Department of Electrical Engineering and Computer Science, University of Michigan, Ann Arbor, MI, USA. He is the lead author of four books: *Theory of Microwave Remote Sensing* (Wiley, 1985) and *Scattering of Electromagnetic Waves* (Vols. 1–3, Wiley, 2001). His current research interests are in remote sensing, random media and rough surfaces, computational electromagnetics, electromagnetic compatibility, and photonic crystals.

Dr. Tsang was the Editor-in-Chief of the IEEE TRANSACTIONS ON GEOSCIENCE AND REMOTE SENSING from 1996 to 2000 and was the President of the IEEE GRSS from 2006 to 2007. He is an honorary life member of GRSS. He has been the Chair of the PhotonIcs and Electromagnetics Research Symposium (PIERS) since 2008. He was a recipient of the Distinguished Achievement Award from GRSS in 2008. He received the Golden Florin Award in 2010, the William Pecora Award co-sponsored by the United States Geological Survey (USGS) and NASA in 2012, the IEEE Electromagnetics Award in 2013, and the van de Hulst Light Scattering Award in 2018. He is a Fellow of the Optical Society of America and a member of the U.S. National Academy of Engineering.

Tianlin Wang (Member, IEEE) received the B.E. degree in electrical engineering from East China University of Science and Technology, Shanghai, China, the M.S. degree in radio physics from Fudan University, Shanghai, China, and the M.S. and the Ph.D. degree in electrical engineering from the University of Michigan, Ann Arbor, MI, USA.

He is currently a postdoctoral scholar in the Department of Electrical and Computer Engineering and ElectroScience Laboratory of The Ohio State University. His research interests include electromagnetic wave theory, microwave remote sensing, microwave measurements, and radio frequency (RF) circuits.

Dr. Wang is a member of Tau Beta Pi, Eta Kappa Nu, the AGU and the Institute of Navigation (ION) and an Early Career Member of Commission F of the United States National Committee (USNC) for URSI. He received the 2018 IEEE Mikio Takagi Student Prize, an Outstanding Student Presentation Award at 2018 AGU Fall Meeting, 2020 Richard F. and Eleanor A. Towner Prize for Distinguished Academic Achievement and Distinguished Leadership Award from the University of Michigan, and the 2021 Ernest K. Smith USNC-URSI Student Prize (2nd Place). He is a recipient of 2020 President's Postdoctoral Scholars Program (PPSP) Fellowship from the Ohio State University and 2021 Mistletoe Research Fellowship from the Momental Foundation.

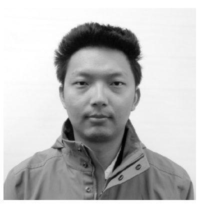

Haokui Xu (Graduate Student Member, IEEE) received the B.S. degree in electrical engineering from the Beijing Institute of Technology, Beijing, China, in 2014 and the M.S. degree from the University of Michigan, Ann Arbor, USA, in 2016, where he is now working towards his Ph.D. degree. His research interests include wave scattering from terrestrial snow, thermal emissions from polar ice sheets, and GNSS-R land applications.

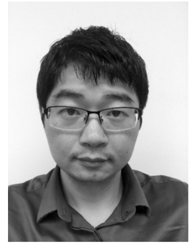

Jiyue Zhu (Student Member, IEEE) received the B.E. degree in electronic and information engineering from Xidian University, Xi'An, China, in 2012 and the M.Sc. degree in electromagnetics and microwave techniques from Southeast University, Nanjing, China, in 2015. He received the Ph.D. degree in electrical engineering from the University of Michigan, Ann Arbor, MI, USA, in 2021. His research interests include wave propagation and scattering for random rough surfaces and random media, and computational electromagnetics in remote sensing for soil moisture and snow.

Mahta Moghaddam (Fellow, IEEE) received the B.S. degree (with Highest Distinction) in electrical and computer engineering from the University of Kansas, Lawrence, KS, USA, in 1986, and the M.S. and Ph.D. degrees in electrical and computer engineering from the University of Illinois at Urbana-Champaign, Urbana, IL, USA, in 1989 and 1991, respectively.

She is Distinguished Professor and the holder of the Ming Hsieh Chair with the Department of Electrical and Computer Engineering of the University of Southern California, Los Angeles, CA, USA. Prior to that, she was a Professor of electrical and computer engineering at the University of Michigan, Ann Arbor, MI, USA, from 2003 to 2011, and with NASA JPL, Pasadena, CA, USA, from 1991 to 2003. She has introduced new approaches for quantitative interpretation of multichannel radar imagery based on analytical inverse scattering techniques applied to complex and random media. She was a System Engineer for the Cassini Radar and was the Science Chair of the JPL Team X (Advanced Mission Studies Team). Her most recent research interests include the development of new radar instrument and measurement technologies for subsurface and subcanopy characterization, development of forward and inverse scattering techniques for layered random media especially for soil moisture and permafrost applications, geophysical retrievals using signal-of-opportunity reflectometry, and transforming concepts of radar remote sensing to medical imaging and therapy systems.

Dr. Moghaddam was a member of the SMAP Mission Science Team and is a member of the CYGNSS Science Team. She was the Principal Investigator of the Airborne Microwave Observatory of Subcanopy and Subsurface (AirMOSS) NASA Earth Ventures 1 Mission and is a member of the National Academy of Engineering.